Design of Wireless Power Smart Personal Protective Equipment for Industrial Internet of Things

IEEE Access
Multidisciplinary ⋮ Rapid Review ⋮ Open Access Journal

Received 20 May 2024, accepted 30 May 2024, date of publication 3 June 2024, date of current version 12 June 2024.

Digital Object Identifier 10.1109/ACCESS.2024.3408915

RESEARCH ARTICLE

Design of Wireless Power Smart Personal Protective Equipment for Industrial Internet of Things

ANDREA BONTEMPI, (Graduate Student Member, IEEE), DANILO DEMARCHI, (Senior Member, IEEE), AND PAOLO MOTTO ROS, (Member, IEEE)
Department of Electronics and Telecommunications (DET), Politecnico di Torino, 10129 Turin, Italy
Corresponding author: Andrea Bontempi (andrea.bontempi@polito.it)

This work was supported by SPAS4S Project.

ABSTRACT Personal Protective Equipment (PPE) is crucial in safeguarding against workplace hazards. However, incidents still occur due to improper PPE usage. With the rise of Industry 4.0 and increasing industrial automation, efforts aim to develop systems for real-time monitoring of PPE. We have developed a proof-of-concept of wireless-powered smart PPE that integrates commercial off-the-shelf electronics with PPE. The smart PPE consists of a power harvesting system, an Ultra-High Frequency Radio-Frequency Identification (UHF RFID) tag for tracking and data communication, and a microcontroller directly supporting capacitive sensing used to recognize the correct wearing of the PPE. A common UHF RFID reader interrogates and powers the smart PPE at the same time using the EPCglobal Class-1 Generation-2 communication protocol. The power harvester is more than 30 % efficient at −10 dBm, and the capacitive measurement shows a peak consumption of less than 100 µA at 1.8 V. Finally, the smart PPE was tested in a realistic scenario. The test was conducted by distancing the smart PPE from the reader from 1 m to 4 m in 1 m steps. The results showed that the wireless power supply and the communication data are feasible up to 4 m. The proposed smart PPE is an ultra-low-power wearable solution that easily integrates into industrial infrastructure and is easily miniaturized, ensuring a significant improvement in workplace safety by enabling real-time monitoring of correct PPE usage.

INDEX TERMS Battery-free smart sensors, industrial Internet of Things, safety management, smart personal protective equipment, wireless power system.

I. INTRODUCTION

Personal Protective Equipment (PPE) safeguards individuals from potential workplace hazards and risks [1]. PPE is defined as any device or accessory that is meant to be worn by employees to protect them from one or more threats that could endanger workplace safety. PPE is a broad category that includes a variety of tools and outfits made to lessen the effects of a variety of risks, such as ergonomic, physical, chemical, and biological dangers. These specialized instruments are essential for establishing a safe working environment, ranging from gloves to helmets and high-visibility vests [2]. Industries identify elevated and reduced risk areas, necessitating workers in these zones to utilize different PPEs adapted to the specific level of necessary protection. Nowadays, ensuring operators use correct PPE remains challenging as inspections primarily rely on human intervention. In [3], four reasons why PPEs are still not correctly used were highlighted. Specifically, the reasons are divided into underestimation of danger, absence of PPE in the work environment, the negative influence of coworkers, and physical discomfort. One of the main issues in the industry safety application is the lack of a system within a workplace that verifies whether

The associate editor coordinating the review of this manuscript and approving it for publication was Alon Kuperman.

the worker is correctly wearing PPE. One solution adopted is to integrate Radio-Frequency Identification (RFID) into PPEs so that the entry and exit of PPE from the work area can be tracked. The works reported in [4], [5], and [6] propose solutions that allow tracking and locating devices using the received signal strength indicator for indoor applications. However, these solutions cannot ensure the operator wears PPE during work activities. Further, RFIDs are increasingly used as sensors even though their applicability in the real world and an industrial scenario is still in question [7]. Research focused on safety and smart PPE is rapidly growing. Indeed, different solutions apply the industrial internet of things concept to wearable sensor systems for industry scenarios [8], [9]. The work described in [10] introduces a prototype of a smart helmet designed to monitor workers' environmental conditions and conduct a near real-time risk assessment using WiFi to exchange data with the centralized server. In work [11], a smart wearable system is developed to monitor cases of epileptic patients working in an industrial environment using WiFi as the transmission method. The work described in [12] proposes a custom, low-power sensors node using various sensors to monitor environmental conditions, particularly air quality. It continuously monitors environmental data in real time and transmits it to a cloud server using LoRa. The work presented in [13] discusses deploying a wearable wireless sensor network to monitor hazardous gases in an industrial environment using an RF transceiver (Xbee) for communication data. Also, the work in [14] uses the same communication method for a sensor node for environmental monitoring.

The main challenge of wearable sensor node systems is the design of an effective, efficient, and safe power supply (eventually including energy storage components) and management systems. Although many proposed solutions require batteries [10], [11], [13], the latter can pose potential hazards in case of malfunction or failure. Battery disposal can be costly and significantly impact the overall life cycle of PPE. To ensure better safety and usability over time, solutions [12], [14] have opted for secondary power supply systems (solar panels), requiring low-power consumption systems with increasingly efficient energy harvesting systems. However, solar panels are difficult to integrate into industrial wearable systems, as they require a continuous light source for proper operation and must be exposed, making them fragile and easily damaged. Additionally, solutions [10], [11], [13], [14] all use active communication systems that require tens of milliamps during transmission, necessitating a large storage capacity (order of Farad), which is also challenging to integrate into a wearable system.

The focus of the paper is on the architectural and system-level design, the realization of a first battery-free proof-of-concept prototype of smart PPE, and its functional validation in a realistic scenario. The novelties introduced by the prototype are as follows:

- Ultra-low-power battery-free wearable device.
- Capacitive sensing to actively monitor the correct use of PPE by the worker in real-time.
- Easy integrated into the industrial infrastructure.

The prototype (Fig. 1) is developed using Commercial Off-The-Shelf (COTS) components. It consists of three main elements: a power harvester operating in the Ultra-High Frequency (UHF) band to ensure device power, a communication system based on an RFID tag, and an Ultra-Low-Power Microcontroller Unit (ULP MCU) to monitor real-time PPE usage through capacitive sensing. The principal challenge is to ensure proper power supply to the system, thereby minimizing the power/energy consumption of each component and maximizing the efficiency of power transmission by focusing particularly on the most critical point, the energy harvester. Minimizing power consumption is essential to ensure proper operation of smart PPE.

The paper is structured as follows: Section II provides an overview of different technologies for realizing smart PPEs, emphasizing the choices to design the smart PPE prototype. Section III is focused on the architectural and system-level design, including hardware design choices and the related firmware/software development, for the transmitter and smart PPE. Section IV describes the experimental and validation tests of the proof-of-concept prototype, focusing mainly on fundamental aspects of the system, ensuring low consumption, energy harvester efficiency, sensor functionality, and testing the complete prototype in a realistic scenario. Section V reports the quantitative results obtained from the experimental tests. Section VI discusses the results, highlighting the prototype's performance with respect to the state-of-the-art. Finally, in section VII, conclusions are drawn, emphasizing the advantages and potential applications of the proposed system.

II. TECHNOLOGY OVERVIEW

Nowadays, there is a strong trend towards designing and implementing devices in the Internet of Things (IoT) field, characterized by compact size, wireless connections, extended autonomy, and low management cost [15]. However, these IoT systems are typically battery-powered. Consequently, all the communication systems involved are oriented towards minimizing power consumption, assuming a power source completely independent of the communication system itself. This category includes systems based on Bluetooth Low-Energy, Zigbee, Ant, and Thread.

Alongside these communication systems, the need to wirelessly transmit energy to power or recharge a battery has emerged. However, typically, these approaches either involve short distances (systems based on inductive or resonant magnetic coupling), mainly used for charging battery-powered devices [16], [17], or utilize a non-electromagnetic wireless transmission approach, such as ultrasonic systems [18]. Although non-electromagnetic wireless systems

are potentially interesting, their actual level of technological maturity and the feasibility of integrating them into other applications still need to be clarified. These technologies often rely on proprietary setups that require the installation of custom devices throughout the working environment. Their performance might be influenced by environmental factors that are not always easy to control (e.g., lighting conditions in outdoor environments) or specific workspace characteristics (presence of acoustic insulation in noisy environments or the need to remain within the line of sight of the lighting source).

On the other side, looking at commercial, proven and widespread solutions, there is also an electromagnetic wireless system for long-distance energy transmission, sometimes operating on the same frequencies as the communication channel. Indeed, RFID, designed to detect and identify objects with radio-frequency devices (transponders or tags) using specific tools or readers, combines bidirectional data and energy transmission in a single solution. Tags use the principle of backscattering to communicate with the reader and consist of varying (and thus encoding data transmission) the electrical/electromagnetic characteristics of the tag in response to interrogation by a reader. Simultaneously, the reader is responsible for powering and modulating (transmitting) data in the same electromagnetic propagation and reading the tag's response regarding variations in electrical/electromagnetic characteristics. The possible electromagnetic couplings between antennas are inductive and radiative, leading to different models and equations and resulting in different operating distances: near-field and far-field, both exploited in different RFID solutions. The choice between the two regimes also depends on the geometric dimensions of the antennas (which can determine the size of the devices) and the frequencies in use. Regarding RFID technology, there are four possibilities [19]: Low Frequency (LF): 125 kHz to 134 kHz; proximity readings for passive tags at the order of a few centimeters. High Frequency (HF): 13.56 MHz; proximity readings for passive tags at the order of (a few) tens of centimeters. UHF: 865 MHz - 928 MHz; long-distance readings. Microwave: 2.4 GHz; long-distance readings. Considering the most suitable technology for the system based on the above information, we can exclude the RFID LF technology as it is not suitable for the desired distances. A similar reasoning applies to RFID HF, which, despite potentially reaching distances of interest, is mainly used for short-range communication, for instance, in smart cards or devices based on near-field communication, where we generally talk about contactless communication rather than wireless. The RFID UHF technology is already widely used in logistics and asset tracking, where a longer range, low production and installation costs, and zero maintenance (thus high adaptability to different operational contexts, including environmental and mechanical constraints) are required. From a distance perspective, it is compatible with the analyzed system. Microwave RFID technology, similar to UHF RFID, can reach long distances using semi-passive or active devices. It should also be considered that the band around 2.4 GHz is already extensively used by other communication systems (Bluetooth, WiFi) and could be a source of interference. In contrast, the band around 900 MHz (UHF RFID) is more free. UHF RFID-based systems allow not only remote power supply at long distances but also localization in an indoor environment of RFID tags [20]. RFID tags utilize the backscattering principle to enable communication with the transmitter without using an active communication method like RF transceivers, thus reducing power consumption. In addition, RFID tags are already widely used in industry [21], making integration of the prototype within the industry infrastructure easier and faster. Therefore, the UHF RFID technology is the best solution for using the same RF source to transmit data and transfer power at the same time. Another interesting use of common RFID tags is that they can be used both for data communication and also as sensors [7]. The antenna itself has a dual function: communication and sensing. The operating principle involves a change in the electrical properties of the sensor antenna (e.g., related to surrounding environmental conditions), corresponding to a change in impedance, which causes a change in the backscatter signal, allowing the reader to decode the information. Several solutions have been presented in the literature for RFID sensors to measure environmental parameters [22], [23] or for structural health monitoring, such as to monitor stress and cracks in materials [24], [25] or corrosive processes [26]. Although these applications are potentially very power-efficient and attractive for the smart PPE application, as only the RFID antenna is used, having an antenna that presents the right trade-off between sensing and communication is still challenging. Communication and sensing capabilities demand opposite requirements. The tag's antenna must be matched with the chip, while sensing requires a continuous variation of the antenna impedance [7].

The design of the smart PPE was mainly focused on the chosen energy source, considering that the power received (P_{Rx}) decreases with the square of the distance (1).

$$P_{Rx}(dB) = P_{Tx} + G_{Tx} + G_{Rx} + 20\log_{10}\left(\frac{\lambda}{4\pi r}\right)^2 \quad (1)$$

P_{Tx} represents the transmitted power, G_{Tx} is the transmitter antenna gain, G_{Rx} is the receiver antenna gain, r is the distance between the two antennas, λ is the wavelength. To ensure a proper power supply for the smart PPE, efficient UHF band power harvesting modules operating with input powers below 100 µW are required. In [27], [28], and [29], the authors emphasize the importance of having an efficient harvesting system, especially when energy harvesting is done by exploiting communication data.

The last part of smart PPE design concerns the system's ability to recognize whether the PPE is worn correctly. Again, choosing the method that allows the lowest consumption is crucial. Different sensors can be utilized to recognize proper PPE usage, primarily falling into two broad categories: opti-

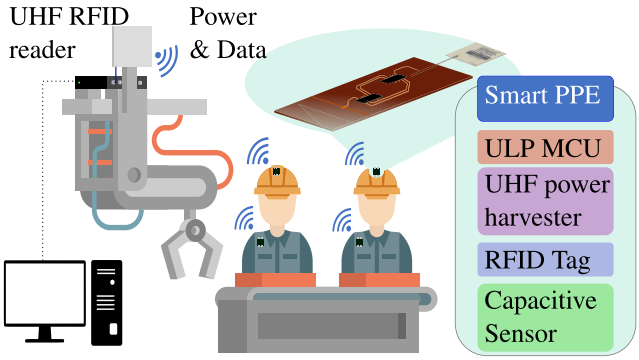

FIGURE 1. New prototype of wearable smart PPE with intelligent sensor technology, fully wirelessly powered to monitor the correct wearing of PPE to reduce hazards. The smart PPE comprises an ultra-low-power microcontroller unit for capacitive sensing, a UHF power harvester, and an RFID tag for data communication with the UHF RFID reader.

cal and mechanical. Optical sensors are extensively applied in the biomedical field, measuring changes in light dispersion and absorption within the body. The main drawback of these sensors is their high energy consumption, posing a significant challenge for fully wireless systems. On the other hand, mechanical sensors, such as piezoresistive, piezoelectric, and capacitive, are also utilized. Different studies [30], [31] have shown that piezoelectric and piezoresistive sensors are highly dependent on environmental conditions, particularly temperature, thus making them unsuitable for industrial applications. Capacitive sensors are widely used to offer an easily realizable solution with a ULP MCU, good sensitivity, and an adaptive sensing configuration [32].

The next section analyzes and describes the architectural and system design to maximize the efficiency of the proposed smart PPE.

III. MATERIALS

A. HARDWARE DESIGN

Fig. 2a shows the assembled prototype of the smart PPE, while fig. 2b represents the hardware configuration in its macro-blocks. The system is divided into two main blocks: the master (transmitter) and the slave (smart PPE). The M6e reader from Thing Magic was chosen for the transmitter, characterized by a maximum deliverable power of 31.5 dBm and capable of handling up to 4 antennas. Two antennas were selected for testing. The first one is the MT-242025 (Mti wireless Edge) with circular polarization and a gain of 7 dBic. The second one is the PA9-12 (Laird) with linear polarization and a gain of 12 dBi.

The smart PPE consists of three main components: the e-peas AEM30940 power harvester, the EM Microelectronic EM4325 tag, and the Texas Instruments MSP430G2553 MCU. COTS components such as AMS SL900A [33] (now discontinued) and Farsens ROCKY100 [34] integrate communication and harvesting functions into a single chip. On the other hand, separating the data communication and the energy harvesting subsystems could allow to specifically optimize and improve the performance of the most critical aspect. To the best of the authors' knowledge, the power harvester e-peas AEM30940 [35] is the one with the lowest cold start equal to 3 µW and here integrated. Exactly for this reason, it was here preferred to the Farsens ROCKY100, which is characterized by a higher input power equal to 177 µW [34]. The configuration of the power harvester is shown in Table 1. A storage capacitor equal to 150 µF was used. The power harvester was configured to ensure capacitor loading to a maximum voltage of 2.7 V and enable LDO at 1.8 V with a maximum deliverable current equal to 80 mA. The maximum power point tracking was set to 50 %.

TABLE 1. Configuration of Power harvester AEM30940.

Description	Name	Configuration	Function
Threshold voltages	CFG[0][1][2]	LLH	Vovch = 2.7 V Vchrdy = 2.3 V Vovdis = 2.2 V Vhv = 1.8 V
MPPT	SELMPP[0][1]	LL	50 %
LDO	ENHV/ENLV	HL	On/Off
Storage capacitor	CBATT	-	150 μF

Symbols used and meaning:
(L) connection to ground, (H) connection to VDD.

The low-power MSP430G2553 MCU was selected for three main reasons: sleep mode consumption is 0.5 µA, it implements an integrated low-power 12 kHz oscillator, and it has an integrated function called "Pin Oscillator" useful for capacitive measurement using only one external electrode [36]. The aluminum foil electrode (4.5 cm × 3.3 cm) is connected to the input of the integrated Schmitt trigger, generating oscillation when the inverted output of the Schmitt trigger is fed back to the input, activating a pull-up or pull-down resistor (Fig. 3). Oscillation frequency decreases when the electrode contacts the tissue due to increased capacitance; thus, it is possible to determine whether the PPE is worn or not. The EM4325 RFID tag is crucial in the proposed smart PPE communication system. The EM4325 tag was used to make the smart PPE recognition unique and ensure communication between the smart PPE and the reader. The tag was chosen because it has a unique Electronic Product Code (EPC) and a Serial Peripheral Interface (SPI) communication peripheral to receive data from the MCU [37]. The registers of the tag were configured, as shown in Table 2. The I/O Control register enables the SPI peripheral in slave mode. Battery management registers 1 and 2 are used to set the read sensitivity of the tag. The chosen mode allows a sensitivity of −28 dBm. The Battery Assisted Passive mode (BAP) is enabled with the register BAP. The communication protocol chosen is the EPCglobal Class-1 Generation-2, so the Tag Only Talk After Listening (TOTAL) register is set to zero.

B. FIRMWARE

The Fig. 2c shows the simplified firmware for the transmitter and smart PPE for data exchange and wireless power

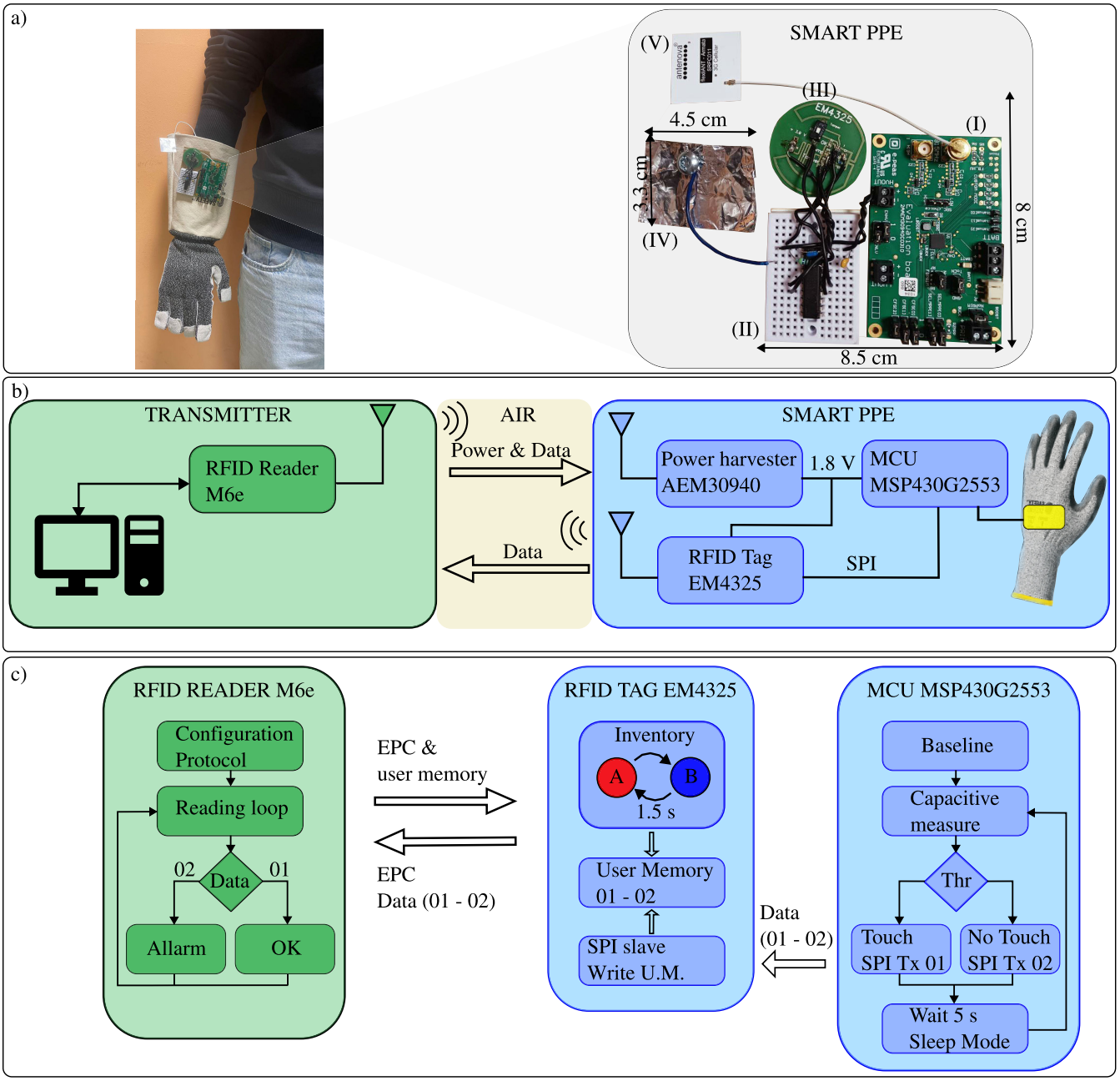

FIGURE 2. a) Proof-of concept of smart PPE. (I) Power harvester AEM30940. (II) ULP MCU MSP430G2553. (III) RFID tag EM4325. (IV) Aluminum electrode foil. (V) SRFC011 UHF antenna. b) Hardware representation of the main macro-blocks for developing smart PPE. c) Overview of the firmware implemented for asynchronous data exchange between the smart PPE and the transmitter (reader).

TABLE 2. Configuration of tag EM4325.

Register	Address (Hex)	Word
I/O Control	F0	2600
Battery Management 1	F1	E001
Battery Management 2	F2	8001
BAP Mode	10D	0001
TOTAL	F3	0000

transmission. A graphical user interface was developed in Visual Studio (1.17.1) for reader configuration and data collection. Mercury application programming interface 1.35.1.103, compatible with firmware 1.25.00.38, provided by Jadak, was used. The reader plays a key role in the proper operation of smart PPE in that it has to ensure a continuous and reliable power supply (for continuous smart PPE sensing) and a proper reading of the monitoring results (stored in the tag's user memory). Using the graphical user interface, it is possible to ensure continuous reading by the reader, thus maximizing the transmitted power and, at the same time, displaying the collected data in real time. The reader

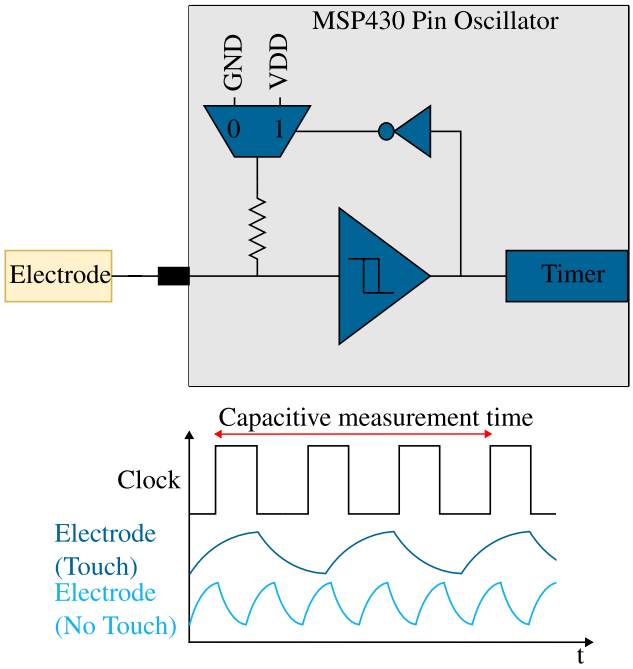

FIGURE 3. MSP430G2553 Pin Oscillator function for capacitive measurement.

is configured using the EPCglobal Class-1 Generation-2 communication protocol. The reading protocol is set to ensure maximum read distance [38] (TARI: 6.25 µs, Encoding: M8, Backscatter Link Frequency (BLF): 250 kHz, Session: S1, Transmitted power: 30 dBm). When the session is set to S1, the tag transitions from state A to state B when read. When the tag is in state B, it cannot be read. The EPCglobal Class-1 Generation-2 standard defines a time span (TS1) in which the tag can remain in state B ranging from 500 ms to 5 s. Each manufacturer decides how long this period should last. For EM4325 tag, the TS1 is ∼1.5 s. With this configuration, the reader continuously requests information from tags, ensuring continuous power supply to the smart PPE. The reader requests the tag identifier (EPC) and the PPE status stored in the tag user memory.

The firmware implemented for the smart PPE manages the capacitive measurement and the writing of the result in the user memory of the tag. As shown in Fig. 3, a time measurement interval is defined in which oscillations (counts) proportional to the change in capacitance of the touchpad (electrode) are counted. At first, the MCU performs a calibration step by repeating the no-load measurement five times, thus defining a baseline due to parasitic capacitances only. Then, the measurement is performed and compared with the baseline by defining delta counts (the difference between measurements and the baseline). An increase in capacitance due to skin contact reduces oscillations (counts) and increases delta counts. If delta counts exceed the set threshold, PPE is worn correctly. Being a threshold on a difference, where one term is the baseline, a fixed threshold can be selected. The capacitive measurement result is written to the tag's user memory using the SPI communication protocol. A 5 s wait time between measurements is set to reduce smart PPE consumption and power supply without sacrificing the overall effectiveness, in terms of safety/security, of the proposed solution. The MCU enters a power-saving state during this period, and the storage capacitor can be recharged.

IV. METHODS

This section describes the test benches used to test the smart PPE. The preliminary tests focus on studying the power harvester, which is crucial in ensuring proper power supply. In parallel, the test bench was prepared to study the power consumption related to the capacitive measurement performed by the MCU to quantify the peak power consumption during the firmware executions and verify whether the capacitive sensing can detect whether the operator is wearing the PPE or not. Finally, a test bench was prepared that simulated realistic conditions to verify the system's correct power supply at different distances and the correct data communication.

A. TEST BENCH FOR POWER HARVESTER EFFICIENCY

The power harvester plays a key role in the proper operation of the device as it manages the power supply to the smart PPE. We tested the AEM30940 power harvester to quantify the efficiency from the input (matching network and rectifier) to the storage capacitor (150 µF). Efficiency was calculated as the ratio of the power required to charge the storage capacitor to the input power (2).

$$\eta = \frac{\frac{0.5 \cdot C \cdot V^2}{\Delta t}}{Pin} \tag{2}$$

In addition, the power harvester wake-up time was measured, which coincides with the time required to charge the storage capacitor to the programmed voltage level. Tests were performed starting from an initial condition characterized by the fully discharged storage capacitor. We applied variable power from −15.5 dBm to 11 dBm in 1.5 Bm steps to the evaluation board input using the RF transmitter (Maxim MAXIM2900) connected to the receiver through a 10 cm coaxial cable to minimize transmission losses; at each repetition, the capacitor was discharged. Both matching networks for low power ("LOW") and high power ("HIGH") of the evaluation board were tested.

Next, the power harvester was tested in more realistic conditions to evaluate the transmitter antenna types and different receiver antenna orientations. The M6e reader was used first with the linear polarization antenna (PA9-12) and then the circular one (MT242025). The helical antenna (ANT-916-CW-RAH) was used for the receiver and was oriented along the three directions (X, Y, and Z). The power harvester was placed at progressively greater distances starting from 2 m to 5 m with a step size of 1 m. Each test was repeated six times.

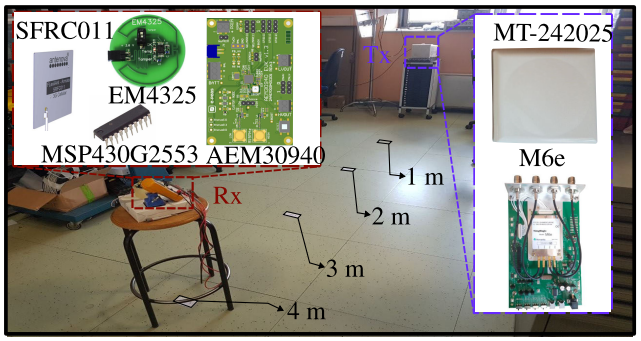

FIGURE 4. Test bench set-up for validation of wireless power and data communication of the smart PPE in a realistic scenario. Four different distances from 1 m to 4 m have been tested, each spaced 1 m.

B. TEST BENCH FOR MCU FIRMWARE CONSUMPTION AND CAPACITIVE MEASUREMENT

The algorithm to detect whether the operator is wearing PPE correctly was performed using an aluminum foil electrode (4.5 cm × 3.3 cm) and six different types of PPE gloves: cut resistant (GDY454 and GDY436), chemical resistant (TL832A), high voltage (GLE36), high temperature (GT300 and GT540W). Different gloves were used to evaluate the algorithm's robustness subjected to different parasitic capacities. Delta counts were collected during the test.

The MCU MSP430G2553 was tested to evaluate its power consumption during capacitive measurement. The Texas Instrument INA240A4, a precision current sensing amplifier with a gain of 200 V/V and a zero current mid-dynamic voltage, was used for the test. The sensing resistance chosen was 15 Ω at 1 % tolerance. The MCU was powered using the Rigol DP832A power supply set to 1.8 V, and current consumption data was collected using the Teledyne LeCroy HD06104 oscilloscope.

C. TEST BENCH FOR SMART PPE IN THE REALISTIC SCENARIO

The proof-of-concept of smart PPE was tested in a realistic scenario to evaluate the feasibility of wireless power supply and data communication with the reader. Fig. 4 shows the test bench; all components are connected as shown in Fig. 2a. The test involves the use of the M6e reader with the Tx antenna MT-242025 and the smart PPE consisting of MSP430G2553 MCU, tag EM4325, and power harvester AEM30940. Two flexible antennas, Armata SRFC011 and Montana SRF21019, were used for the power harvester, characterized by a gain of 2.46 dBi and 1.9 dBi, respectively. The reader was configured to have an output power of 30 dBm. Each test was repeated six times, and the total duration for each measurement was 2 min. During this time, the following parameters were tracked: the number of responses obtained by the tag (EPC and User memory) and the number of measurements completed by the MCU. The MCU performs a measurement every 5 s if properly powered; hence, the maximum number of measurements in two minutes is 24. The tag, set in session S1, is available for reading every 1.5 s, resulting in a maximum of 80 readings in two minutes, in the case of correct power supply and reading.

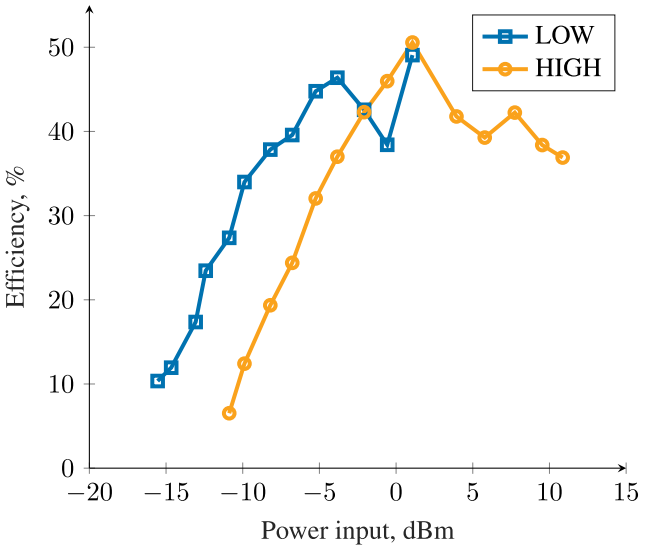

FIGURE 5. Comparison of power harvester AEM30940 efficiency versus input power using two different input impedance matching networks, one for low power ("LOW") and the other for high power ("HIGH").

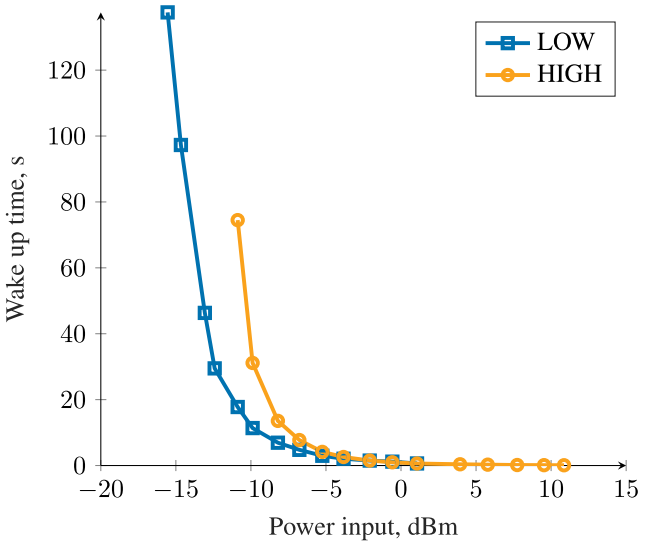

FIGURE 6. Comparison of power harvester AEM30940 wake-up time versus input power using two different input impedance matching networks one for low power ("LOW") and the other for high power ("HIGH").

V. RESULTS

A. POWER HARVESTER EFFICIENCY

The power harvester efficiency and wake-up time results are reported in Fig. 5 and 6, respectively. The efficiency results (Fig. 5) show that for powers less than −2 dBm, the "LOW" matching network exhibits higher efficiency than the "HIGH" matching network, which performs better for higher input powers. The efficiency remains above 30 % up to

input powers of −10 dBm for the "LOW" matching network while for the "HIGH" matching network at least −5 dBm is required to have the same efficiency. For the "LOW" matching network, the minimum measured efficiency is 10 % for a power of −15.5 dBm while the maximum efficiency is 49 % at 1 dBm. For the "HIGH" network, the minimum measured efficiency is 6.5 % at −11 dBm and a maximum of 50 % at 1 dBm.

The wake-up time results (Fig. 6) shows the time required to charge the storage capacitor to the set voltage. As reported in the efficiency results, the "LOW" matching network provides faster charging than the "HIGH" matching network. In particular, for a power of −10 dBm the wake-up time is about 10 s and 30 s ("LOW" and "HIGH"). For lower input powers, the charging time increases exponentially. For the "LOW" matching network, a time of more than 2 min was measured for powers below −15 dBm. For the "HIGH" one, charging could not be completed for powers below −11 dBm. For input powers greater than −3 dBm, both matching networks' measured wake-up time is a few seconds.

Fig. 7 shows the results for wake-up times using a helical antenna (ANT-916-CW-RAH) connected to the input of the power harvester and using two different antennas for the reader (PA9-1 and MT-242025). The results obtained using the linearly polarized antenna (PA9-1) show promising results only when the two antennas are oriented along the direction of maximum gain (Z), obtaining wake-up times of less than 10 s for distances between 2 m and 4 m. While with the Rx antenna oriented along the Y and X axis, the best measured times are 20 s (2 m) and 75 s (2 m) respectively. The results obtained with the circularly polarized antenna (MT-24025) show the best results with the antenna oriented along the X axis with wake-up times ranging from 6 s (2 m) to 15 s (5 m). With the antenna oriented along the Y axis, the measured times range from 11 s (2 m) to 30 s (5 m). While with the antenna oriented along the Z axis, the longer time of 45 s (2 m) was measured.

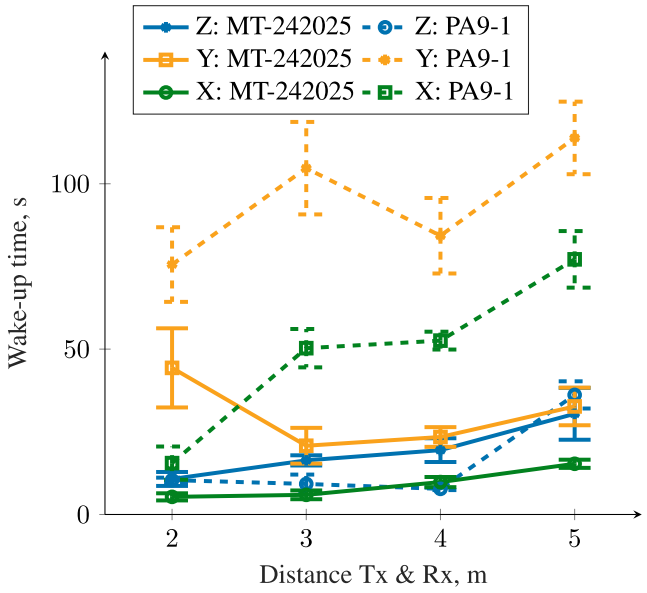

FIGURE 7. Power harvester AEM30940 wake-up time using a helical RX antenna (ANT-916-CW-RAH) and two different TX antennas (MT-242025 circular polarization and PA9-1 linear polarization). The RX antenna was oriented along the X, Y, and Z axes.

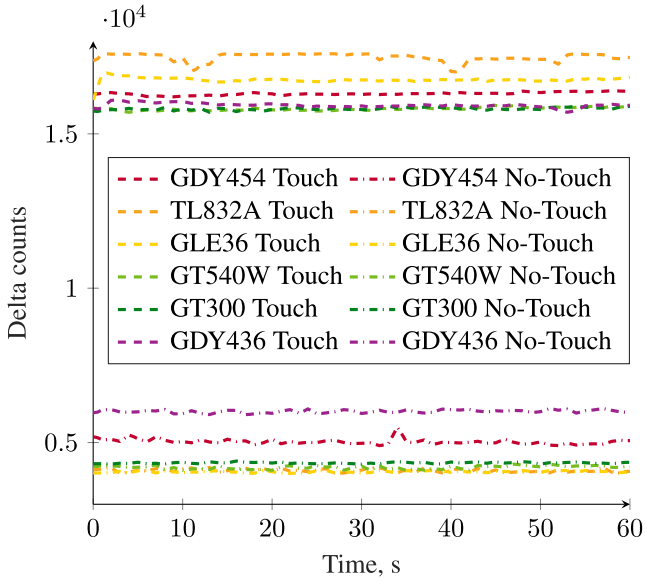

FIGURE 8. Performance of the MSP430G2553 MCU algorithm for recognizing the correct use of PPE. Six different PPE gloves were used for the test.

B. CAPACITIVE MEASUREMENT AND CURRENT CONSUMPTION

The delta counts related to the capacitive measurements are shown in Fig. 8. As evidenced by the results, there is a clear difference between the two conditions tested (worn and unworn PPE). When the worker wears different PPEs, the delta counts are between 16000 and 18000. When the operator is not wearing the PPE, the delta counts are between 4000 and 6000. The power consumption associated with the capacitive measurement is significant in ensuring effective power provisioning for smart PPE. Fig. 9 shows the current consumption of the capacitive measurement. Different phases are evident during the measurement. In the initial phase, the MCU is in sleep mode. Triggered by a temporal interrupt, the MCU transitions to an active state, enabling the requisite registers for capacitive measurement. During this phase, the current consumption is approximately 60 µA. Upon initiating the capacitive measurement, a transient peak current below 100 µA is measured. Transitioning to the subsequent phase, wherein the oscillation counting transpires, the MCU adopts an energy-efficient mode with a reduced consumption of approximately 40 µA. Following the completion of the capacitive measurement, a secondary peak current, also below 100 µA, is shown. The two peaks of 100 µA are due to overlapping consumption due to firmware execution and measurement consumption. In the final phase of the process, the current consumption is ascribed to the data transmission

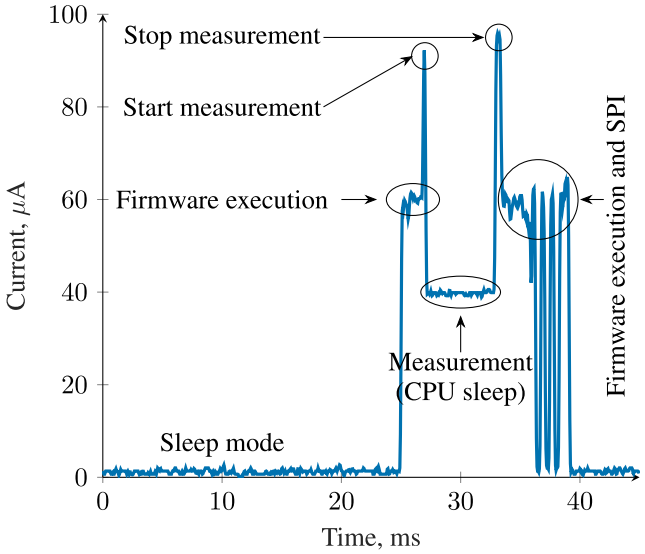

FIGURE 9. Current consumption of MSP430G2553 MCU during capacitive measure.

through SPI. Inter-byte transmission intervals allow the MCU to enter a power-saving state, thereby minimizing energy consumption. Upon the conclusion of data transmission, the MCU reverts to the initial sleep mode. The duration of the capacitive measurement with data transmission lasts 14 ms.

C. SMART PPE RESULTS IN REALISTIC SCENARIO

Fig. 10 shows the mean and standard deviation of the measurements obtained in the realistic scenario test for two different flexible antennas (Armata SRFC011 and Montana SRF2I019). Specifically, the mean and standard deviation of the number of responses obtained by the tag and the number of measurements done by the MCU. The horizontal lines indicate the maximum number of tag responses and MCU measurements obtainable in 2 minutes of testing (80 and 24, respectively). The tests were repeated six times for each distance. The results of the Armata SRFC011 antenna are presented in Fig. 10a, wherein it is observed that up to a distance of 2 m, the reader identified the tag on to the PPE, attaining nearly the maximum conceivable reading count. This trend is mirrored in the count of measurements executed by the MCU, which underscores that the wireless power supply ensures the necessary energy for proper operation. Conversely, at greater distances of 3 m and 4 m, the system's performance exhibits increased variability, however, guaranteeing the power supply of the smart PPE. The reader performed an average of 21 measurements, while the MCU completed an average of 13 at 3 m. While at 4 m, the reader completed an average of 26 readings, and the MCU completed an average of 15. The outcomes associated with the Montana SRF2I019 antenna are presented in Fig. 10b. Similar to the prior case, the most favorable results are achieved at closer distances, specifically at 1 m and 2 m. The

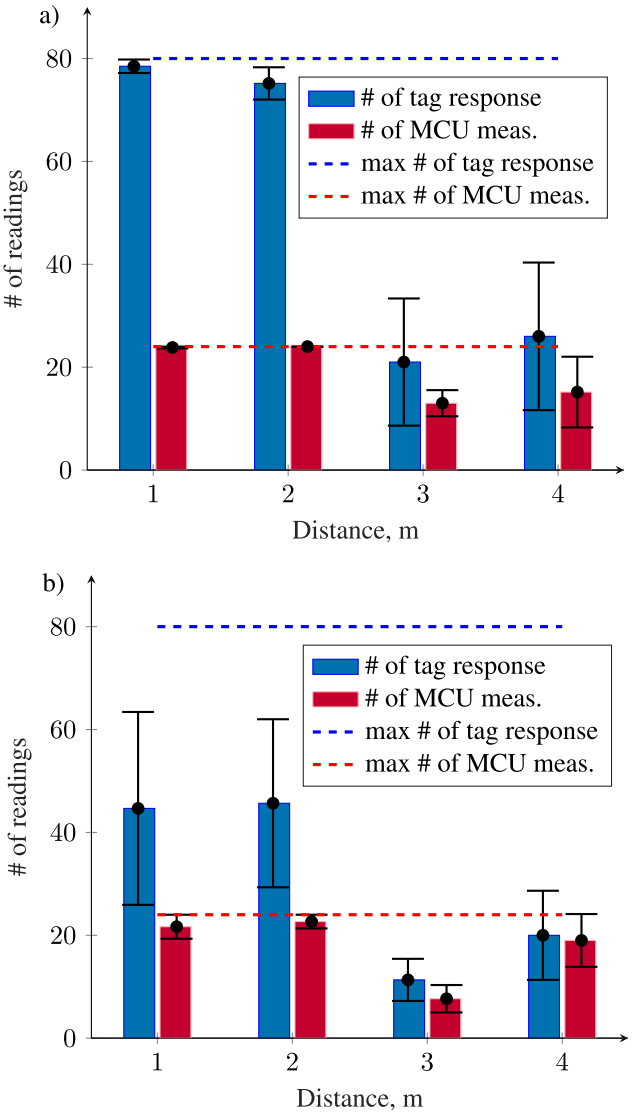

FIGURE 10. Experimental results of smart PPE in a realistic scenario. The mean and standard deviation of the number of responses obtained from the tag (blue), the number of measurements made by the MCU (red). The test was run for 2 min and repeated six times for each distance. In two minutes, the maximum number of readings is 80 (blue dashed line), while the maximum number of MCU measurements is 24 (red dashed line). a) Results were obtained using the Armata SRFC011 flexible antenna. b) Results were obtained using the Montana SRF2I019 flexible antenna.

reader's recorded readings stand at 44 and 45 at 1 m and 2 m, respectively, while the MCU conducted 23 and 24 measurements correspondingly. At 3 m and 4 m, the performance of the system with the Montana SRF2I019 is degraded; however, the system is correctly powered during the tests. The MCU performed 8 and 19 measurements, and the reader recorded values of 11 and 20 at 3 m and 4 m, respectively. The results obtained using the smart PPE in the realistic scenario showed that the system is sufficiently robust even with two different flexible antennas, showing the system's proper operation regarding alimentation and data exchange. Among the two antennas tested, the Armata SRFC011

antenna showed better behavior with less variability, thus showing more robustness for the application and industry environment.

VI. DISCUSSION

The experimental tests have highlighted the main characteristics of the proposed smart PPE, focusing on architectural and system-level design to maximize power harvester efficiency, minimize consumption, and ensure proper prototype operation in a realistic scenario at different distances from the transmitter. The tests on the power harvester have shown the requirements for the correct functioning of the prototype, emphasizing the importance of selecting the matching network and antennas to maximize power harvester efficiency. The ''LOW'' matching network has proven to be more suitable compared to the ''HIGH'' network as it exhibits better performance with lower input powers: 30 % efficiency (Fig. 5) and a 10 s (Fig. 6) wake-up time at −10 dBm. This allows for a quick system startup, as in the case of a completely discharged storage capacity (i.e., in the worst case), the power harvesting system would only take 10 s to recharge it and power the rest of the system (tag and MCU). It is a key aspect for ensuring real-time monitoring. Another crucial aspect is that Rx antennas could potentially have any spatial orientation, mostly not fixed but depending on the use of the PPE. The tests with antennas have highlighted that to ensure power supply in various spatial orientations, the best solution lies with circularly polarized antennas for Tx and linearly polarized antennas for Rx. The results (Fig. 7) show more uniform and lower wake-up times than linear-linear coupling. The smart PPE must ensure sufficiently low power consumption so as not to drain storage capacity during capacitive measurement. The energy consumed by the smart PPE is obtained from the integral of the current consumption (Fig. 9) and multiplied by the supply voltage (1.8 V), which is ∼1.2 µJ. The 150 µF storage capacitor stores ∼546 µJ. The capacitive measurement thus decreases the voltage on the storage capacitor by ∼126 mV, thus ensuring the system's proper operation. During the standby mode of 5 s, the capacitor is recharged to return to the nominal set voltage. It also tested the algorithm's robustness using six types of gloves characterized by different materials. The results (Fig. 8) show two clusters identifying whether the worker was wearing PPE or not.

Finally, the proof-of-concept of the smart PPE was validated with a test bench simulating a realistic condition. This test compared two flexible antennas (Armata SRFC011 and Montana SRF2I019) mounted on the power harvester. The results (Fig. 10) show that the Armata SRFC011 antenna outperforms the Montana SRF2I019 antenna, ensuring proper functionality (power supply and data exchange) up to a distance of 4 m. The best results were obtained up to a distance of 2 m. While for longer distances 3 m to 4 m, the system continues to operate, facilitating data exchange; however, the results also highlight increased variability. This behavior stems from the fact that at distances of 3 m to 4 m, the input power to the smart PPE may not always be sufficient to maintain device operation. Consequently, the device may not be adequately powered, causing the power harvester to temporarily disconnect the power supply to the MCU and the tag. One possible solution is to increase the time between measurements to allow proper charging of the storage capacitor. Also, the reader configuration with only one antenna was used in the measurement setup, but extending its operation to 4 antennas is possible, ensuring greater spatial coverage.

Table 3 compares this work concerning the state-of-the-art smart devices for PPE and industry safety. The table shows different solutions using primary or secondary power systems and active or passive transmission systems. Our system, as well as the one in [40], compared to the state-of-the-art, presents a solution that leverages the same energy source for both powering and data communication, ensuring better compactness by avoiding the use of a primary power source (battery) [10], [11], [13], [39] and enabling potential system miniaturization on flexible substrates. Battery-powered systems require continuous maintenance due to replacement or recharging of the batteries themselves, unlike systems using secondary power that are immediately ready for use. The reported battery lifespan in [13] and [39] are 10 h and 384 h, respectively. In contrast, systems that use a secondary power system are immune to this issue by ensuring immediate use and an infinite device lifetime. Batteries can overheat or short-circuit, especially if damaged or misused, thus increasing the risk of serious accidents, especially in sensitive or hazardous work environments. The proposed system guarantees power consumption at least three orders of magnitude lower than those reported in [12], [13], and [14] and an order of magnitude lower compared to the system in [40]. The key advantage of using a single capacitive sensor and backscattering as the communication method is the reduction in power consumption while still ensuring the monitoring of proper PPE usage. Furthermore, compared to systems powered by a secondary power source [12], [14], the storage capacity is significantly lower, further enabling improved system miniaturization. A key aspect of the proposed system is to provide greater spatial coverage. The systems presented in [13] and [14] have significantly greater coverage because they use an active transmission method; on the other hand, the power consumption is significantly higher, thus having to rely on either a primary power system or a secondary power system and big supercapacitor, making the systems impractical to the wearable. In comparison, the system presented in [40], albeit with similar characteristics, shows an operational range smaller by almost a factor of 3 with a single transmitter antenna and the same output power equal to 30 dBm. Specifically, our system can support smart PPE up to 4 m, whereas the maximum distance in [40] is limited to 1.5 m. Extending the reader's operation to utilize multiple antennas could enhance spatial coverage. In [40], it is estimated that by using

TABLE 3. State-of-the-art of smart PPE for safety applications.

Ref.	Sensors	Maximum Current [mA]	Maximum Power [mW]	Power Supply	Lifespan [h]	Storage Capacitor [F]	Wireless Protocol	Maximum Distance [m]
[10]	Gas Temperature Humidity Luminosity Accelerometer	N/A	N/A	Battery Lithium 3.7 V	N/A	Not Used	WiFi	N/A
[11]	ECG, EEG, NIMB, GPS, Accelerometer	N/A	N/A	Battery	N/A	Not Used	WiFi	N/A
[39]	CO_2, O_2, H_2S, Temperature, Accelerometer	7.51	24.78	Battery, Lithium Polymer, 3.3 V, 380 mAh	384	Not Used	BLE	N/A
[13]	CO_2, IRC-A1, Temperature, Humidity	160	592 #	Battery, Lithium Polymer, 3.7 V, 800 mAh	10	Not Used	LR-WPAN	50*
[14]	CO_2, UV Humidity Temperature	48	154	Solar cell	∞	12	LoRa	520
[12]	CO_2, Humidity, Temperature	165	515	Solar cell	∞	50	LR-WPAN	N/A
[40]	Capacitive	1	2.2	UHF harvester	∞	100×10^{-6}	UHF RFID	1.5 - 50†
This work	**Capacitive**	**0.1**	**0.18**	**UHF harvester**	∞	**150×10^{-6}**	**UHF RFID**	**4**

* Multiple antennas. # Retrieved from the paper infromations. † Simulated results with multiple antennas.

more readers, it is possible to extend the coverage range up to 50 m.

The potential of our system is the realization of a ULP wearable system that can be easily integrated into the industrial infrastructure and miniaturized, which can, at the same time, improve workplace safety by actively monitoring the proper use of PPE in real time.

VII. CONCLUSION

In this work, the proof-of-concept of a smart PPE has been introduced. The system allows for real-time monitoring of whether the PPE is worn correctly by the worker, ensuring enhanced industrial safety, ease of integration, and miniaturization. Compared to the state-of-the-art, this system reduces power consumption by at least three orders of magnitude and leverages simultaneous wireless information and power transfer. The proposed system offers numerous advantages, including increased safety in hazardous environments, greater adherence to safety protocols, and the potential to prevent accidents and injuries. Real-time monitoring facilitates timely interventions and corrective measures promoting a safer work environment. In future work, we will focus on the miniaturization of the system to integrate it into flexible substrates, enhancing its versatility and adaptability. We also envision implementing multiple transmitting TX antennas to enhance the system's spatial coverage, track the status of PPE, and localize the position within the workplace. In addition, the experimental tests will be extended in real scenarios of work environments, allowing for a comprehensive assessment of its effectiveness and reliability.

ACKNOWLEDGMENT

The authors would like to thank Lanzi Group and Mect Mechatronic Thinking for their technical support.

REFERENCES

[1] T. Gammon, W.-J. Lee, Z. Zhang, and B. C. Johnson, "'Arc flash' hazards, incident energy, PPE ratings and thermal burn injury—A deeper look," *IEEE Trans. Ind. Appl.*, vol. 51, no. 5, pp. 4275–4283, Apr. 2015.

[2] Europa Agency for Safety and Health at Work. (2020). *Smart Personal Protective Equipment: Intelligent Protection for the Future*. Accessed: Nov. 11, 2024. [Online]. Available: https://osha.europa.eu/sites/default/files/Smart_personal_protective_equipment_intelligent_protection_of_the_future.pdf

[3] T. K. M. Wong, S. S. Man, and A. H. S. Chan, "Critical factors for the use or non-use of personal protective equipment amongst construction workers," *Saf. Sci.*, vol. 126, Jun. 2020, Art. no. 104663.

[4] M. Omer and G. Y. Tian, "Indoor distance estimation for passive UHF RFID tag based on RSSI and RCS," *Measurement*, vol. 127, pp. 425–430, Oct. 2018. [Online]. Available: https://www.sciencedirect.com/science/article/pii/S0263224118305207

[5] C. Peng, H. Jiang, and L. Qu, "Deep convolutional neural network for passive RFID tag localization via joint RSSI and PDOA fingerprint features," *IEEE Access*, vol. 9, pp. 15441–15451, 2021.

[6] T. Montanaro, I. Sergi, A.-T. Shumba, M. Pizzolante, M. Pirozzi, and L. Patrono, "BLE-based IoT proximity warning system for guaranteeing the operators' safety in outdoor working environments," in *Proc. 8th Int. Conf. Smart Sustain. Technol. (SpliTech)*, Jun. 2023, pp. 1–6.

[7] J. Zhang, G. Tian, A. Marindra, A. Sunny, and A. Zhao, "A review of passive RFID tag antenna-based sensors and systems for structural health monitoring applications," *Sensors*, vol. 17, no. 2, p. 265, Jan. 2017. [Online]. Available: https://www.mdpi.com/1424-8220/17/2/265

[8] S. Misra, C. Roy, T. Sauter, A. Mukherjee, and J. Maiti, "Industrial Internet of Things for safety management applications: A survey," *IEEE Access*, vol. 10, pp. 83415–83439, 2022.

[9] C. Arcadius Tokognon, B. Gao, G. Y. Tian, and Y. Yan, "Structural health monitoring framework based on Internet of Things: A survey," *IEEE Internet Things J.*, vol. 4, no. 3, pp. 619–635, Jun. 2017.

[10] I. Campero-Jurado, S. Márquez-Sánchez, J. Quintanar-Gómez, S. Rodríguez, and J. Corchado, "Smart helmet 5.0 for industrial Internet of Things using artificial intelligence," *Sensors*, vol. 20, no. 21, p. 6241, Nov. 2020. [Online]. Available: https://www.mdpi.com/1424-8220/20/21/6241

[11] A. Hayek, S. Telawi, J. Börcsök, R. Abi Zeid Daou, and N. Halabi, "Smart wearable system for safety-related medical IoT application: Case of epileptic patient working in industrial environment," *Health Technol.*, vol. 10, no. 1, pp. 363–372, Jan. 2020, doi: 10.1007/s12553-019-00335-2.

[12] F. Wu, C. Rüdiger, and M. Yuce, "Real-time performance of a self-powered environmental IoT sensor network system," *Sensors*, vol. 17, no. 2, p. 282, Feb. 2017. [Online]. Available: https://www.mdpi.com/1424-8220/17/2/282

[13] D. Antolín, N. Medrano, B. Calvo, and F. Pérez, "A wearable wireless sensor network for indoor smart environment monitoring in safety applications," *Sensors*, vol. 17, no. 2, p. 365, Feb. 2017. [Online]. Available: https://www.mdpi.com/1424-8220/17/2/365

[14] F. Wu, J.-M. Redouté, and M. R. Yuce, "WE-safe: A self-powered wearable IoT sensor network for safety applications based on LoRa," *IEEE Access*, vol. 6, pp. 40846–40853, 2018.

[15] J. Henkel, S. Pagani, H. Amrouch, L. Bauer, and F. Samie, "Ultra-low power and dependability for IoT devices (invited paper for IoT technologies)," in *Proc. Design, Autom. Test Eur. Conf. Exhib.*, 2017, pp. 954–959.

[16] F. Del Bono, A. Bontempi, A. Dentis, N. Di Trani, D. Demarchi, A. Grattoni, and P. M. Ros, "Design of a closed-loop wireless power transfer system for an implantable drug delivery device," *IEEE Sensors J.*, vol. 24, no. 6, pp. 7345–7354, Mar. 2024.

[17] K. Agarwal, R. Jegadeesan, Y.-X. Guo, and N. V. Thakor, "Wireless power transfer strategies for implantable bioelectronics," *IEEE Rev. Biomed. Eng.*, vol. 10, pp. 136–161, 2017.

[18] S. H. Song, A. Kim, and B. Ziaie, "Omnidirectional ultrasonic powering for millimeter-scale implantable devices," *IEEE Trans. Biomed. Eng.*, vol. 62, no. 11, pp. 2717–2723, Nov. 2015.

[19] D. M. Dobkin, "Chapter 2—History and practice of RFID," in *The RF in RFID*, D. M. Dobkin, Ed., 2nd ed. Waltham, MA, USA: Newnes, 2013, pp. 7–47. [Online]. Available: https://www.sciencedirect.com/science/article/pii/B9780123945839000028

[20] Z. Wei, J. Chen, H. Tang, and H. Zhang, "RSSI-based location fingerprint method for RFID indoor positioning: A review," *Nondestruct. Test. Eval.*, vol. 39, no. 1, pp. 3–31, Jan. 2024, doi: 10.1080/10589759.2023.2253493.

[21] J. C. S. dos Santos, F. O. O. Gomes, M. A. ds Santos, M. C. F. de Castro, N. Grando, R. Travessini, and R. S. Weirich, "Optimized ultra-low power sensor-enabled RFID data logger for pharmaceutical cold chain," in *Proc. IEEE Brazil RFID*, Oct. 2015, pp. 1–5.

[22] J. Virtanen, L. Ukkonen, T. Bjorninen, A. Z. Elsherbeni, and L. Sydänheimo, "Inkjet-printed humidity sensor for passive UHF RFID systems," *IEEE Trans. Instrum. Meas.*, vol. 60, no. 8, pp. 2768–2777, Aug. 2011.

[23] S. Manzari, C. Occhiuzzi, S. Nawale, A. Catini, C. Di Natale, and G. Marrocco, "Humidity sensing by polymer-loaded UHF RFID antennas," *IEEE Sensors J.*, vol. 12, no. 9, pp. 2851–2858, Sep. 2012.

[24] P. Kalansuriya, R. Bhattacharyya, and S. Sarma, "RFID tag antenna-based sensing for pervasive surface crack detection," *IEEE Sensors J.*, vol. 13, no. 5, pp. 1564–1570, May 2013.

[25] X. Yi, C. Cho, J. Cooper, Y. Wang, M. M. Tentzeris, and R. T. Leon, "Passive wireless antenna sensor for strain and crack sensing—Electromagnetic modeling, simulation, and testing," *Smart Mater. Struct.*, vol. 22, no. 8, Jul. 2013, Art. no. 085009, doi: 10.1088/0964-1726/22/8/085009.

[26] A. I. Sunny, G. Y. Tian, J. Zhang, and M. Pal, "Low frequency (LF) RFID sensors and selective transient feature extraction for corrosion characterisation," *Sens. Actuators A, Phys.*, vol. 241, pp. 34–43, Apr. 2016. [Online]. Available: https://www.sciencedirect.com/science/article/pii/S0924424716300668

[27] K. W. Choi, S. I. Hwang, A. A. Aziz, H. H. Jang, J. S. Kim, D. S. Kang, and D. I. Kim, "Simultaneous wireless information and power transfer (SWIPT) for Internet of Things: Novel receiver design and experimental validation," *IEEE Internet Things J.*, vol. 7, no. 4, pp. 2996–3012, Apr. 2020.

[28] S. K. Divakaran and D. D. Krishna, "RF energy harvesting systems: An overview and design issues," *Int. J. RF Microw. Comput.-Aided Eng.*, vol. 29, no. 1, Jan. 2019, Art. no. e21633.

[29] K. Lee and J. Ko, "RF-based energy transfer through packets: Still a dream? Or a dream come true?" *IEEE Access*, vol. 7, pp. 163840–163850, 2019.

[30] F. Baptista, D. Budoya, V. Almeida, and J. Ulson, "An experimental study on the effect of temperature on piezoelectric sensors for impedance-based structural health monitoring," *Sensors*, vol. 14, no. 1, pp. 1208–1227, Jan. 2014.

[31] K. J. Suja, G. S. Kumar, R. Komaragiri, and A. Nisanth, "Analysing the effects of temperature and doping concentration in silicon based MEMS piezoresistive pressure sensor," *Proc. Comput. Sci.*, vol. 93, pp. 108–116, Jan. 2016.

[32] J. Heikenfeld, A. Jajack, J. Rogers, P. Gutruf, L. Tian, T. Pan, R. Li, M. Khine, J. Kim, J. Wang, and J. Kim, "Wearable sensors: Modalities, challenges, and prospects," *Lab Chip*, vol. 18, no. 2, pp. 217–248, 2018.

[33] (2018). *SL900A EPC Gen2 Sensor Tag*. [Online]. Available: https://ams-osram.com/products/interfaces/sensor-interfaces/ams-sl900a-epc-gen2-sensor-tag

[34] (2017). *EPC C1G2 Compliant UHF RFID Tag With Power Harvesting SPI Commun. for External Low Power Sensors Actuators*. Accessed: Mar. 5, 2024. [Online]. Available: http://www.rtutech.com/28web/Upload/20181225105747967.pdf

[35] (2023). *Highly Efficient, Regulated Dual-Output, Ambient Energy Manager for AC or DC Sources With Optional Primary Battery*. [Online]. Available: https://e-peas.com/product/aem30940/

[36] (2022). *MSP430F2xx, MSP430G2xx Family User's Guide*. Texas Instruments. [Online]. Available: https://www.ti.com/product/MSP430G2553

[37] (2023). *18000-63 Type C (Gen2) 18000-63 Type C/18000-64 Type D (Gen2/TOTAL) RFID IC*. [Online]. Available: https://www.emmicroelectronic.com/product/epc-and-uhf-ics/em4325

[38] (2020). *Mercury API Programmer's Guide*. Jadak. Accessed: Apr. 18, 2024. [Online]. Available: https://www.jadak.com.cn/upload/product/thingmagicmercuryapichengxuyuanzhinan.pdf

[39] R. De Fazio, A.-R. Al-Hinnawi, M. De Vittorio, and P. Visconti, "An energy-autonomous smart shirt employing wearable sensors for users' safety and protection in hazardous workplaces," *Appl. Sci.*, vol. 12, no. 6, p. 2926, Mar. 2022. [Online]. Available: https://www.mdpi.com/2076-3417/12/6/2926

[40] S. He, J. Chen, F. Jiang, D. K. Y. Yau, G. Xing, and Y. Sun, "Energy provisioning in wireless rechargeable sensor networks," *IEEE Trans. Mobile Comput.*, vol. 12, no. 10, pp. 1931–1942, Oct. 2013.

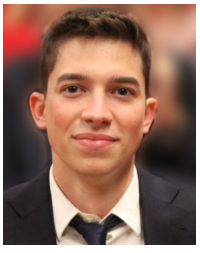

ANDREA BONTEMPI (Graduate Student Member, IEEE) received the B.Sc. and M.Sc. degrees in biomedical engineering from Politecnico di Torino, in 2018 and 2021, respectively. He is currently pursuing the Ph.D. degree with the Department of Electronics and Telecommunication (DET), Electronic Life-Oriented iNtelligent Systems (eLiONS) Research Group.

Since 2021, he has been the Treasurer of the IEEE Student Branch, Politecnico di Torino. His research interests include electronic and microelectronic system applied to biomedical devices.

DANILO DEMARCHI (Senior Member, IEEE) was a Visiting Professor with Tel Aviv University, from 2018 to 2021, and EPFL Lausanne, in 2019. He was a Visiting Scientist with MIT and Harvard Medical School, in 2018, for the project Smart electronic IoT SysTEms for Rehabilitation sciences (SISTER). He is currently a Full Professor with the Department of Electronics and Telecommunication, Politecnico di Torino. He is Leading the electronic Life-Oriented iNtelligent Systems (eLiONS) Laboratory, Politecnico di Torino, and coordinating Italian Institute of Technology Microelectronics Group, Politecnico di Torino (IIT@DET). He is the author and coauthor of five patents and more than 300 scientific publications in international journals and peer-reviewed conference proceedings. His research interests include micro and nano electronics, smart system integration, and the IoTs for the agrifood value chain and for biomedical devices.

He was a member of the IEEE Sensors Council, from 2020 to 2023, and the BioCAS Technical Committee, since 2013. He was the General Chair of the IEEE Biomedical Circuits and Systems Conference (BioCAS), Turin, in 2017 and a Founder of the IEEE FoodCAS Workshop (Circuits and Systems for the FoodChain); the TPC Co-Chair of IEEE ICECS 2019, IEEE BioCAS 2021, and IEEE BioCAS 2022 conferences; the General Co-Chair of the IEEE BioCAS 2023. He is a Founder and the Chair of the IEEE CAS Special Interest Group on AgriFood Electronics (CAFE). He is a Founder and the Vice-Chair of the IEEE CAS Special Interest Group on AgriFood Electronics. He is an Associate Editor of IEEE Open Journal on Engineering in Medicine and Biology (OJ-EMB). He is a Founder and the Editor-in-Chief of IEEE Transactions on AgriFood Electronics (TAFE). From 2023 to 2024 a Distinguished Lecturer of the IEEE CAS Society with the Lecture ''Let the Plants Do the Talking: Smart Agriculture by the messages received from Plants and Soil''.

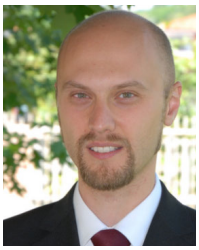

PAOLO MOTTO ROS (Member, IEEE) received the M.Sc. and Ph.D. degrees in electronic engineering from Politecnico di Torino, Italy, in 2005 and 2009, respectively.

He was a Postdoctoral Researcher with Politecnico di Torino, Turin, Italy, from 2009 to 2012, a Senior, since 2014, Postdoctoral Researcher with Istituto Italiano di Tecnologia, from 2012 to 2019, a Senior Postdoctoral Researcher, from 2019 to 2022, and an Adjunct Professor, since 2017, with Politecnico di Torino. He is currently an Assistant Professor with the Department of Electronics and Telecommunication, Politecnico di Torino. He is the author and coauthor of more than 80 international scientific publications.

Dr. Motto Ros was a member of the organizing committee of IEEE ICECS 2019, the FoodCAS Satellite Event at IEEE ISCAS 2021, and IEEE CAFE 2023; a Review Committee of IEEE BioCAS 2021-2024, a Special Session Organizer at IEEE MeMeA 2021, a Program Committee Member of IEEE LASCAS 2022 and 2023. He was Program Co-Chair of ApplePies 2024. He was Guest Editor of MDPI Sensors, and a Guest Associate Editor of Frontiers in Neurorobotics. He is Associate Editor of IEEE Transactions on Biomedical Circuits and Systems and IEEE Transactions on AgriFood Electronics.

Open Access funding provided by 'Politecnico di Torino' within the CRUI CARE Agreement